

## Supporting Information for

# **Nucleation management for ambient fabrication of high-performance perovskite photodetectors with eco-friendly tert-butanol anti-solvent**

Xin Tang,<sup>‡</sup> Tengteng Li,<sup>‡</sup> Qingyan Li, Hongliang Zhao, Silei Wang, Mengyao Li, Xuanruo Hao, Yating Zhang,<sup>\*</sup> Jianquan Yao<sup>\*</sup>

Key Laboratory of Opto-Electronics Information Technology, Ministry of Education, School of Precision Instruments and Opto-Electronics Engineering, Tianjin University, Tianjin 300072, China

<sup>‡</sup>This authors contributed equally to this work

<sup>\*</sup>Corresponding author: yating@tju.edu.cn

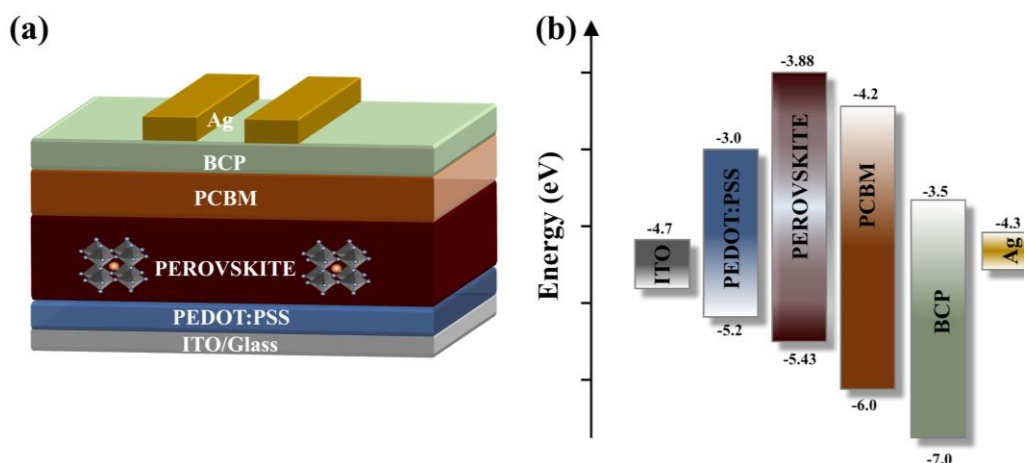


Figure S1 (a) Schematic device structure of PPDs. (b) The schematic energy level diagram of PPDs.

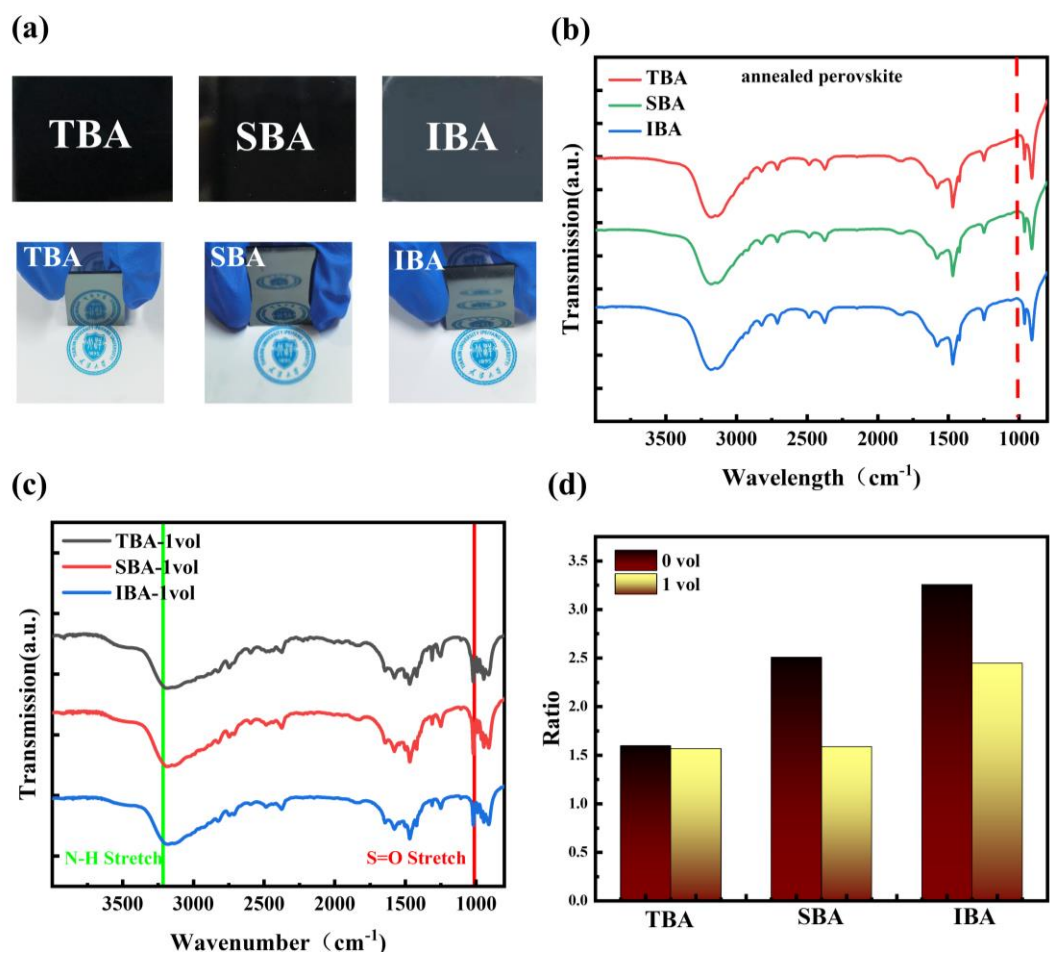


Figure S2. (a) The direct view and corresponding mirror-like effect image of perovskite films prepared by different anti-solvent after annealing. (b) FTIR spectra of MAPbI<sub>3</sub> perovskite prepared by TBA, SBA, and IBA with annealing; (c) FTIR spectra of MAPbI<sub>3</sub> perovskite prepared by the water-doped antisolvents without annealing; (d) The ratio of the absorbance intensity of the unannealed perovskite films with pure TBA, SBA, and IBA at 0 vol and 1 vol.

anti-solvents and water-doped antisolvents at  $1020$  and  $3200\text{ cm}^{-1}$  ( $1020\text{ cm}^{-1}$ : $3200\text{ cm}^{-1}$ ).

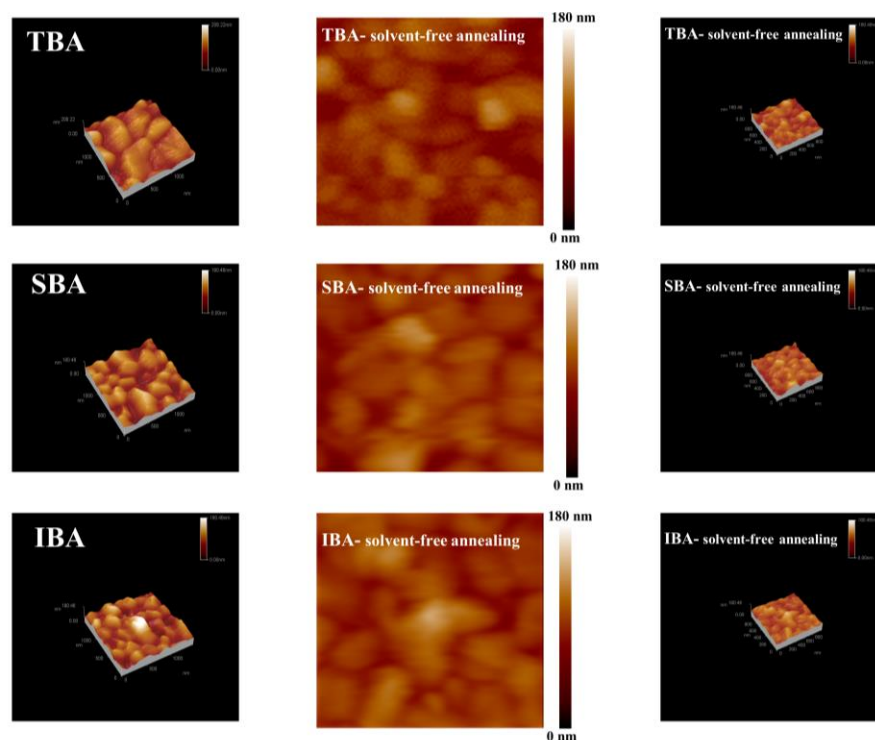


Figure S3. (a) 3D-AFM images obtained from TBA-PVK, SBA-PVK, and IBA-PVK; (b) AFM images corresponding to TBA-PVK, SBA-PVK, and IBA-PVK with solvent-free annealing. The scanning range of the images is  $1\ \mu\text{m} \times 1\ \mu\text{m}$ ; (c) 3D-AFM images obtained from TBA-PVK, SBA-PVK, and IBA-PVK with solvent-free annealing.

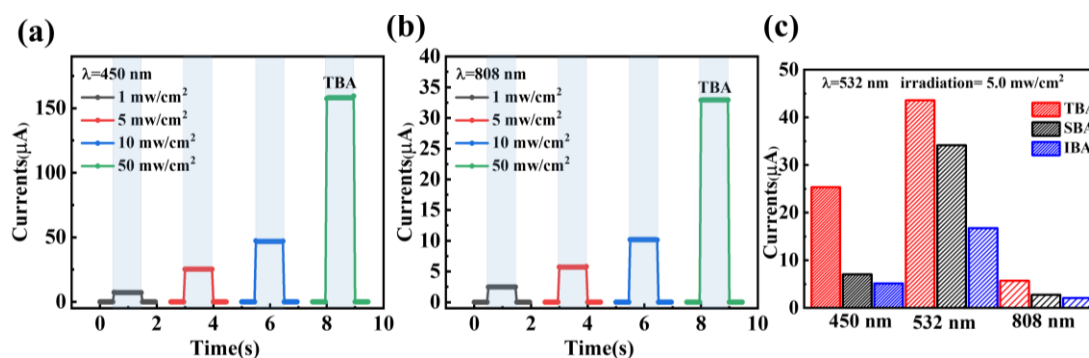


Figure S4. Part electrical and optical switching characteristics of TBA-PD. (a) Photoswitching characteristics under 450 nm laser illumination with different power densities ( $V_{\text{Bias}} = 0\text{ V}$ ); (b) Photoswitching characteristics under 808nm laser illumination with different power densities ( $V_{\text{Bias}} = 0\text{ V}$ ). (c) Photocurrent distribution

histogram corresponding to the results in Figure 5f.

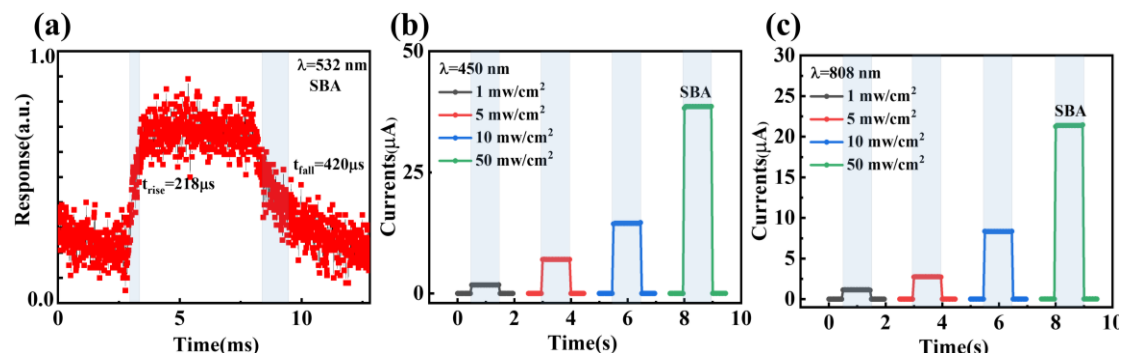


Figure S5. Part electrical and optical switching characteristics of SBA-PD. (a) Response time measurement under one on-off illumination cycle of the 532 nm laser with a pulse frequency of 100 Hz.; (b) Photoswitching characteristics under 450 nm laser illumination with different power densities ( $V_{\text{Bias}} = 0$  V); (c) Photoswitching characteristics under 808 nm laser illumination with different power densities ( $V_{\text{Bias}} = 0$  V).

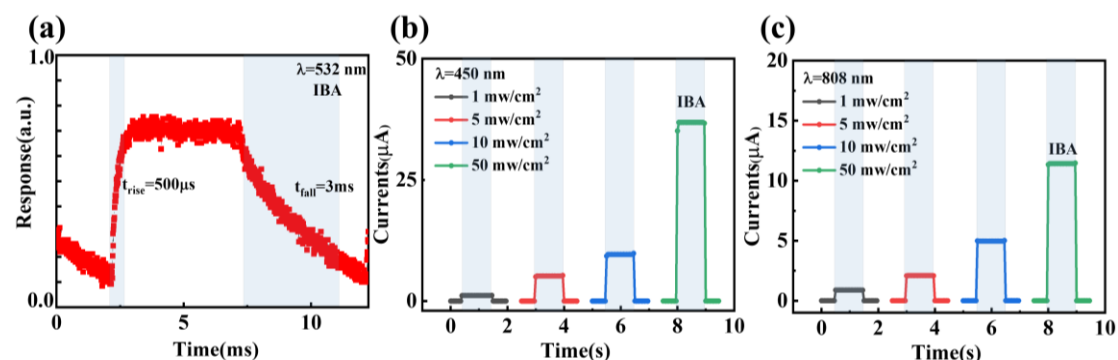


Figure S6 Part electrical and optical switching characteristics of IBA-PD. (a) Response time measurement under one on-off illumination cycle of the 532 nm laser with a pulse frequency of 100 Hz; (b) Photoswitching characteristics under 450 nm laser illumination with different power densities ( $V_{\text{Bias}} = 0$  V); (c) Photoswitching characteristics under 808 nm laser illumination with different power densities ( $V_{\text{Bias}} = 0$  V).